Effect of SiO_2 nanoparticles on the hydrophobic properties of waterborne fluorine-containing epoxy coatings

Xiaofang Liu[1, a], Rongwei Wang[1], Yongkang Fan[1], Ming Wei[1]

[1]*School of Chemistry, Chemical Engineering and Life Sciences, Wuhan University of Technology, 430070 Wuhan, Hubei, China*

Abstract. A nano-composite coating was developed by adding nano-SiO_2 to a home-made Waterborne fluorine-containing epoxy resin. The surface hydrophlicity of the coating was investigated by the contact angle with water. As the particle sizes of SiO_2 changed from 7-18nm, the water contact angle of the films changed from 62.8° to 85.6°. The surface energy of the coating was calculated out through measuring the contact angles of the coating with water and 1-bromonaphthalene. The presence of SiO2 significantly enhanced the corrosion resistance of the composite coatings, which showed two times than that of the neat waterborne fluorine-containing epoxy coatings. And the thermos dynamic stability of the composite coatings has been significantly improved. When the silica content is 2.0%, the coating has the largest contact angle. Other performance of the coating was investigated in terms of their thickness, flexibility, pencil hardness, impact resistance.

1 Introduction

Hydrophobic coatings create an attractive interest both in industry and academia due to their unique self-cleaning properties as a result of their water repelling character[1]. Based on the lotus leaf effect and other natural phenomena[2-6], highly hydrophobic surfaces have been prepared by roughening low surface energy materials. The chemical composition of a coating determines its surface free energy. The C-F bond is a kind of the strong organic bonds[7].The introduction of fluorinated component to the coating is an effective method to improve water impermeability and reduce surface free energy on the architecture of the molecular structure, which will increase the hydrophobic properties of coatings because of their small dipole and the low polarizability of the C–F bond together with the large free volume[8-9]. Various techniques have been applied to increase the surface roughness, including plasma etching [10-12], electrochemical deposition[13-14], chemical vapor deposition[15-16], nanoparticles deposited[17-18], etc. Meanwhile the addition of nanoparticles such as nano-Ti [19], nano-SiO_2[20], nano-ZnO[21-22] increase of the corrosion resistance.

In the present work, we modified waterborne fluorine-containing epoxy coatings with different contents of SiO_2 nanoparticles and different particle sizes. This study aims to make a hydrophobic coating from the SiO_2 nanoparticles as deposit sediment to improve the roughness. And anticorrosion properties of modified waterborne fluorine-containing epoxy coatings were also studied.

2 Experimental

2.1 Materials

SiO_2 nanoparticles(A380, A300, A200, A150, S103583) was purchased from Evonik and Aladdin company，with the particle sizes of 7, 9, 12, 14, and 18nm. 1-bromonaphthalene and NaCl were purchased from Aladdin Industrial Corporation. Waterborne fluorine-containing epoxy resin was home-made its structure is shown in Fig.1 and waterborne epoxy curing agent 8545 was supplied by Momentive Performance Materials Company. Defoaming agent, leveling agent, corrosion inhibitor agent, wetting and dispersing agent were obtained from Elementis-specialties.

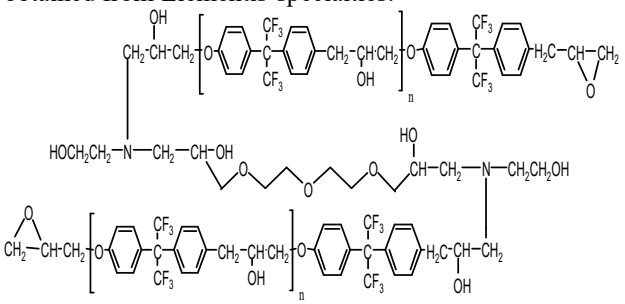

Fig.1 the structure of waterborne fluorine-containing epoxy resin

2.2 Preparation of waterborne fluorine-containing epoxy coatings

[a] Corresponding author: Xiaofang Liu@sdjclxf@sina.com

The epoxy emulsion was prepared by the waterborne fluorine-containing epoxy resin, SiO_2 nanoparticles and deionized water via phase inversion method (75℃, 3000 rpm, high speed dispersers.) with a solid content of 50% and average particle size of 75.8 nm. The deionized water dropped into the system at a speed of 1 mL/min. The waterborne fluorine-containing epoxy coating was obtained by mixed waterborne fluorine-containing epoxy emulsion, waterborne epoxy curing agent and defoaming agent, leveling agent, corrosion inhibitor agent, wetting and dispersing agent evenly. In the waterborne epoxy coating, the ratio of epoxy and amine hydrogen is controlled as 1:0.5, and the total content of leveling agent, corrosion inhibitor agent and wetting and dispersing agent are 0.2wt%, together with the defoaming agent content of 0.4wt %.

2.3 Measurement and Characterization

Surface water contact angles of coatings were studied by contact angle measuring instrument (JC2000C3, Chengdu best instrument Co., China). The surface energy of the coating is calculated through the Owens-Wendt-Kaelble theory[23-24] . The corrosion resistance of coating was studied by EIS (AUTOLAB PGSTAT30, Metrohm Co., Switzerland). The thermal gravimetric analysis of coating was studied by TG-DSC (STA449F3, Netzsch Co., Germany). Coatings were applied on previously sanded tinplates. After drying, the coating properties such as: bending test[25], adhesion test[26], impact[27], scratch hardness by pencil test[28], were determined by standard methods. The thickness of the film was measured by coating thickness gauges (QNIX4500, QNIX Co., Germany).

3 Results and Discussion

3.1 Effect of the particle sizes of SiO_2 on the water contact angles of coatings

The influences of the particle sizes of SiO_2 on the water contact angles of coatings are illustrated in Fig 2, with the constant of 1 wt % SiO_2 nanoparticles.

The SiO_2 addition with different particle sizes affected the water contact angles of coatings. The minimum contact angle is 62.8°while the largest is 85.6°. The water resistance of the paint film is mainly determined by two factors: the structure and the solid surface energy of the paint film. The different particle sizes of SiO_2 could make different scales of structure.

3.2 Effect of the contents of SiO2 nanoparticl

-es on the water contact angles of coatings

With the choose of 18 nm SiO_2, the effect of SiO_2 (S103583) contents on water contact angles for coatings was investigated, as shown in Fig. 3 The water contact angles of the composite coatings gradually increased with the content of SiO_2 increased from 0.5 to 2.0wt %. Specifically, the introduction of 1.5wt% and 2.0wt% SiO_2 nanoparticles significantly advanced the hydrophobicity of the composite coatings, which induced the water contact angles of coatings higher than 90°. However, an excess of SiO_2 addition caused the decrease of the water contact angles, because a small amount of SiO_2 were exposed to the outer edge of the paint film. The exposed hydrophilic SiO_2 results in the decrease of the hydrophobic of the paint film .When the content of SiO_2 is higher than 1.5wt%, the viscosity of emulsion has increased dramatically, and presents a paste. When the content of SiO_2 was 2.0wt % the advantage of the hydrophobic effect is not obvious compared with 1.5 wt%. Taking the coating process and the hydrophobic effect into consideration, we chose 1.5wt% as an appropriate content.

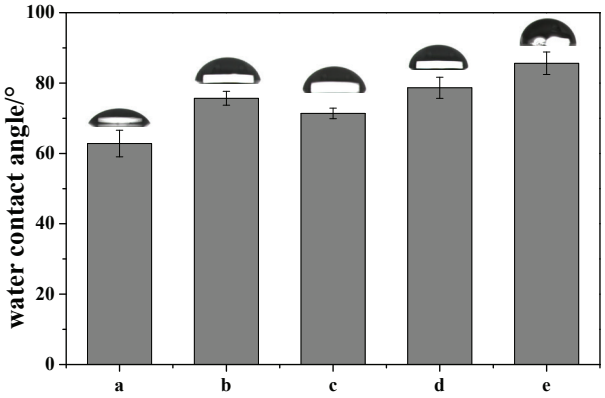

Fig.2 Water contact angles of coatings with different particle sizes of SiO_2

Table 1. Water contact angles of coatings with different particle sizes of SiO_2

Code	a	b	c	d	e
Particle sizes of SiO_2/nm	7	9	12	14	18
Contact angle(°)	62.8 ±3.8	75.7 ±2.0	71.4 ±1.5	78.7 ±3.0	85.6 ±3.2

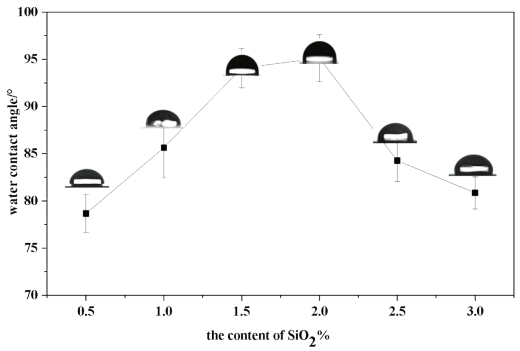

Fig.3 Water contact angles of coatings with different contents of SiO_2

3.3 Evaluation of comprehensive performanc-e of the coating

3.3.1 Surface energy of the coating

The surface energy of solids is an important index to evaluate its' hydrophobic properties. Deionized water and

1-bromonaphthalene were used for the contact angles measurement of the composite coatings. The surface tension and its components for water and 1-Bromonaphthalene are listed in Table 2. The γ_{lv}, γ_{plv} and γ_{dlv} represent the surface tension the polar and nonpolar component of the liquid. The contact angles of coating with the water and 1-bromonaphthalene were shown in Fig. 4, which exhibited the values of 94.06° (water) and 53.5° (1-bromonaphthalene). According to Eq. (2), the surface energy of the coating was calculated as 29.93 mN/m.

$$\gamma_{lv}(1+\cos\theta) = 2\sqrt{\gamma_{sv}^{d}\gamma_{lv}^{d}} + 2\sqrt{\gamma_{sv}^{p}\gamma_{lv}^{p}} \quad (1)$$

γ_{sv}^{p}=1.57 γ_{sv}^{d}=28.36

$$\gamma_{sv} = \gamma_{sv}^{p} + \gamma_{sv}^{d} = 1.57 + 28.36 = 29.93 \quad (2)$$

Table 2. Surface tension and its components for water and 1-Bromonaphthalene

Liquid	γ_{lv}(mN/m)	γ_{lv}^{p}(mN/m)	γ_{lv}^{d}(mN/m)
Water	72.8	51.0	21.8
1-Bromonaphthalene	44.6	0	44.6

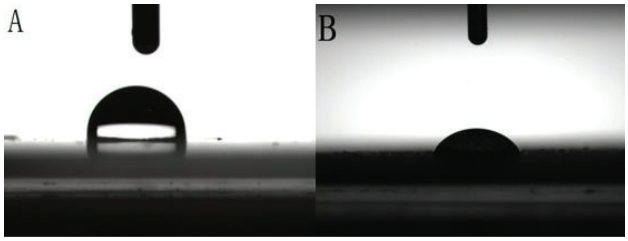

Fig.4 (A) Water contact angle of coating (B) 1-Bromonaphthal-Ene contact angle of the coating

3.3.2 The corrosion resistance of the coatings

Electrochemical Impedance Spectroscopy (EIS) measurement was used to investigate the corrosion resistance of the samples. Electrochemical measurements were conducted using a three electrode system. The fluorine-containing epoxy-coated steel coupon served as the working electrode, while the counter electrode and the reference electrode used were a platinum grid and a saturated calomel electrode respectively. The EIS experiment was performed at room temperature in aqueous 3.5 wt% NaCl solution prepared by dissolving sodium chloride in deionized water. The steel was polarized at ±10 mV around its open circuit potential by an alternating current signal with its frequency ranging from 10^{5}Hz to 10^{-2}Hz. Fig. 5 was the nyquist diagram of EIS test. Z´ and Z " represents the real and imaginary parts of the impedance, respectively. The result of the coating contained SiO2 was curve A and curve B was the fitted value by using the equivalent circuit shown in Fig.6. The result of coating without SiO2 was curve C and curve D was the fitted value by using the equivalent circuit shown in Fig.7. The measured curves basically are consistent with the calculated curves, and thus the fitted value can better reflect the real situation. It could be seen that the incorporation of SiO_2 increased the coating resistance obviously and improved the quality of the cured epoxy coating. The calculated resistance of the coating contained SiO_2 was 64909 Ω·cm^2. The calculated resistance of the coating without SiO_2 was 35990 Ω·cm^2. The addition of SiO_2 improved nearly twice corrosion resistance of the coating.

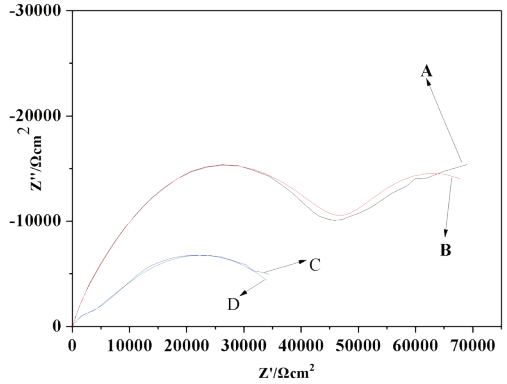

Fig.5 EIS Nyquist diagram for fluorine-containing epoxy-coated steel after 7 days (A) measured value with SiO2 in the coating (B) fitted value(C) measured value without SiO2 in the coating (D) fitted value

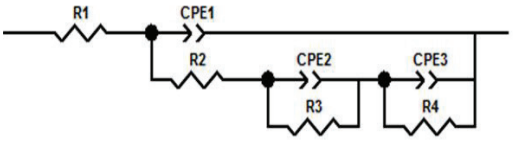

Fig.6 Schematic drawing of the equivalent circuit. R1 is associated with the electrolyte resistance. R2 and CPE1 are the resistance and capacitance of Outer layer including the passivation film and corrosion products etc, respectively. R3 and CPE2 are the resistance and capacitance of coating porosities, respectively. CPE3 is the capacitance of the double layer. R4 is the charge transfer resistance.

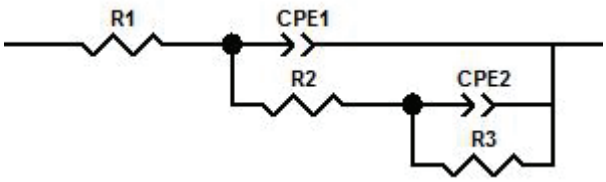

Fig.7 Schematic drawing of the equivalent circuit . R1 is associated with the electrolyte resistance. R2 and CPE1 are the resistance and capacitance of Outer layer including the passivation film and corrosion products etc, respectively. CPE2 is the capacitance of the double layer. R3 is the charge transfer resistance.

3.3.3 The thermal gravimetric (TG) analysis of coating

The thermal properties of the coating were studied by the TG-DSC, which is used to analyze the degradation steps and thermal stability of epoxy resin coatings. Fig. 8 A, B displays TG weight loss and weight loss derivative curves in air. The DTG curve clearly indicated that the coating underwent four main degradation stages. The first stage was the volatilization of residuary water, in the temperature range of 20-250 ℃. The second stage from 250 to 380 ℃ was the thermal degradation process of the low crosslinking density of curing products and some

monomer resin, curing agent not involved in the curing reaction. The third stage, between 380 and 470℃, was the thermal degradation process of side chain and end group of the skeleton structure. The final process was the degradation of the skeleton structure in the temperature range of 470-670℃.

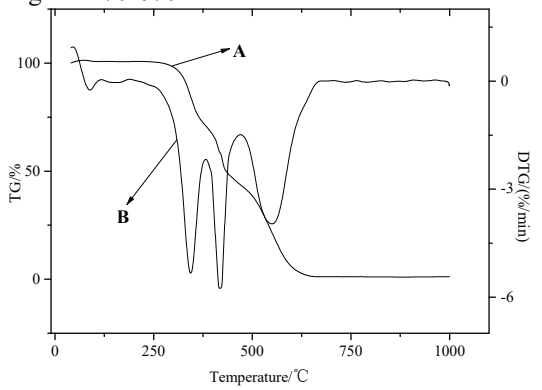

Fig.8 Thermogravimetric and Derivative curves of coating (A) TG (B) DTG

The comprehensive performances of the waterborne fluorine-containing epoxy coating loaded with 1.5 wt% SiO_2 nanoparticles (18 nm) are listed in Table 3, which shows the promising surface hydrophobicity, high corrosion resistance, and excellent.

Table.3 Comprehensive performances of waterborne fluorine-containing epoxy coating.

Performances	Results
Resistance/Ω·cm^2	64909
Contact angel/°	94.1±2.1
Thickness/(μm)	48.7
Flexibility/(mm)	2
Adhesion/(grade)	1
Pencil hardness/H	3
Impact resistance/(kg.cm)	50

4 Conclusions

The waterborne fluorine-containing epoxy coatings modified by SiO_2 nanoparticles showed a higher contact angle. With the presence of 18 nm SiO_2 nanoparticles at the loading level of 1.5wt%, the coating exhibited the hydrophobic property from and the water contact angle of 94.1°. The surface energy of the coating is calculated as 29.9 mN/m. The hydrophilic-to-hydrophobic transition of fluorine-containing epoxy coating derived from the interaction of low surface energy and SiO_2 nanoparticles. The addition of SiO_2 improved corrosion resistance of the coating obviously, and the coating showed a good thermodynamic stability.

References

1. Liu X, Liang Y, Zhou F, et al. Extreme wettability and tunable adhesion: biomimicking beyond nature [J]. Soft Matter, 2012, 8(7): 2070-2086.
2. Sun, T.; Feng, L.; Gao, X; et al. Bioinspired surfaces with special wettability [J]. Acc. Chem. Res. 2005, 38, 644-652.
3. Hosono, E.; Fujihara, S.; Honma, I.; et al. Superhydrophobic perpendicular nanopin film by the bottom-up process [J]. Am. Chem. Soc. 2005, 127, 13458-13459.
4. Zhang, X.; Shi, F.; Niu, J.; et al. Superhydrophobic surfaces: From structural control to functional application [J]. Mater. Chem.2008, 18, 621-633.
5. Wenzel R N. Surface Roughness and Contact Angle [J]. The Journal of Physical Chemistry, 1949, 53(9): 1466-1467.
6. Nishino T, Meguro M, Nakamae K, et al. The lowest surface free energy based on-CF3 alignment [J]. Langmuir, 1999, 15(13): 4321-4323.
7. Lee J R, Jin F L, Park S J, et al. Study of new fluorine-containing epoxy resin for low dielectric constant [J]. Surface and Coatings Technology, 2004, 180: 650-654.
8. Merkel T C, Toy L G. Comparison of hydrogen sulphide transport properties in fluorinated and nonfluorinated polymers [J]. Macromolecules, 2006, 39(22): 7591-7600.
9. Tao Z, Yang S, Ge Z, et al. Synthesis and properties of novel fluorinated epoxy resins based on 1, 1-bis (4-glycidylesterphenyl)-1-(3′-trifluoromethylphenyl)-2, 2, 2-trifluoroethane[J]. European polymer journal, 2007, 43(2): 550-560.
10. Jin M, Feng X, Xi J, et al. Super-hydrophobic PDMS surface with ultra-low adhesive force[J]. Macromolecular rapid communications, 2005, 26(22): 1805-1809.
11. Balu B, Breedveld V, Hess D W. Fabrication of "roll-off" and "sticky" superhydrophobic cellulose surfaces via plasma processing [J]. Langmuir, 2008, 24(9): 4785-4790.
12. Fernández-Blázquez J P, Fell D, Bonaccurso E, et al. Superhydrophilic and superhydrophobic nanostructured surfaces via plasma treatment[J]. Journal of colloid and interface science, 2011, 357(1): 234-238.
13. Wang M F, Raghunathan N, Ziaie B. A nonlithographic top-down electrochemical approach for creating hierarchical (micro-nano) superhydrophobic silicon surfaces [J]. Langmuir, 2007, 23(5): 2300-2303.
14. Jiang Y, Wang Z, Yu X, et al. Self-assembled monolayers of dendron thiols for electrodeposition of gold nanostructures: toward fabrication of superhydrophobic/superhydrophilic surfaces and pH-responsive surfaces[J]. Langmuir, 2005, 21(5): 1986-1990.
15. Intranuovo F, Sardella E, Rossini P, et al. PECVD of fluorocarbon coatings from hexafluoropropylene oxide: glow vs. afterglow [J]. Chemical Vapor Deposition, 2009, 15(4-6): 95-100.
16. Li S, Li H, Wang X, et al. Super-hydrophobicity of large-area honeycomb-like aligned carbon nanotubes[J]. The journal of physical chemistry B, 2002, 106(36): 9274-9276.
17. Kylián O, Polonskyi O, Kratochvíl J, et al. Control of Wettability of Plasma Polymers by Application of Ti Nano-Clusters [J]. Plasma Processes and Polymers, 2012, 9(2): 180-187.

18. Solař P, Kylián O, Polonskyi O, et al. Nanocomposite coatings of Ti/C: H plasma polymer particles providing a surface with variable nanoroughness [J]. Surface and Coatings Technology, 2012, 206(21): 4335-4342.
19. Zhang X Z, Li Y J. Effects of Nano-sized Titanium Powder on the Anti-corrosion Property of Epoxy Coatings on Stee l[J]. Kemija u industriji, 2014, 63(9-10): 317-322.
20. Sadreddini S, Salehi Z, Rassaie H. Characterization of Ni–P–SiO2 nano-composite coating on magnesium [J]. Applied Surface Science, 2015, 324: 393-398.
21. Ramezanzadeh B, Attar M M. Studying the effects of micro and nano sized ZnO particles on the corrosion resistance and deterioration behavior of an epoxy-polyamide coating on hot-dip galvanized steel [J]. Progress in Organic Coatings, 2011, 71(3): 314-328.
22. Duraibabu D, Ganeshbabu T, Manjumeena R, et al. Unique coating formulation for corrosion and microbial prevention of mild steel[J]. Progress in Organic Coatings, 2014, 77(3): 657-664.
23. Owens D K, Wendt R C. Estimation of the surface free energy of polymers[J]. Journal of applied polymer science, 1969, 13(8): 1741-1747.
24. Kaelble D H. Dispersion-polar surface tension properties of organic solids[J]. 1970, 2(2): 66-81.
25. Standard Test Method for Bend Test, China Standard Specification, GB1731-79.
26. Standard Test Method for Adhesion, China Standard Specification, GB 1720-79.
27. Standard Test Method for Impact, China Standard Specification, GB/T 1732-1993.
28. Standard Test Method for Coating Hardness by Pencil Test, China Standard Specification, GB/T 6739-2006.